International Journal of Heat and Mass Transfer 115 (2017) 926–931

Contents lists available at ScienceDirect

International Journal of Heat and Mass Transfer

journal homepage: www.elsevier.com/locate/ijhmt

Condensation heat transfer in a sessile droplet at varying Biot number and contact angle

Sanjay Adhikari, Mahdi Nabil, Alexander S. Rattner *

Department of Mechanical and Nuclear Engineering, The Pennsylvania State University, University Park, PA 16802, United States

ARTICLE INFO

Article history:
Received 17 February 2017
Received in revised form 13 July 2017
Accepted 14 July 2017

Keywords:
Dropwise condensation
Conduction heat transfer

ABSTRACT

Dropwise condensation has been identified as a promising heat transfer mechanism because it can yield heat fluxes up to an order of magnitude higher than typically found in filmwise condensation. Models for dropwise condensation generally assume a statistical distribution of droplet sizes and integrate heat transfer over the droplet size spectrum, considering droplet curvature effects on saturation temperature, conduction thermal resistance, and interfacial resistance. Most earlier studies have assumed a constant heat transfer factor ($f = O(1)$) to account for the conduction contribution to total thermal resistance. However, f varies with droplet Biot number (Bi) and contact angle (θ). Formulations for f with broad ranges of applicability are not currently available. In this study, finite element simulations are performed to determine f and corresponding numerical uncertainties for $0.0001 \leqslant \mathrm{Bi} \leqslant 1000$ and $10^\circ \leqslant \theta \leqslant 170^\circ$. This spans the active droplet size range considered in most droplet condensation studies (*e.g.*, for water condensing at P_{atm} on a surface 10 K below the ambient temperature, active droplets have $0.0005 < \mathrm{Bi} < 300$). An explicit correlation is proposed for f and is validated with published results. The proposed correlation can facilitate modeling and analysis of dropwise condensation.

1. Introduction

Dropwise condensation has been identified as a promising high-flux heat transfer mechanism for applications in power generation [1], desalination [2], and electronics thermal management [3]. Dropwise condensation often yields heat transfer rates up to an order of magnitude higher than that filmwise condensation [4,5]. The dropwise condensation process initiates from minute primary droplets (<1 μm diameter) at discrete nucleation sites distributed over a cooled surface [6,7]. Droplets with a radius greater than the minimum thermodynamically viable radius [4,8] grow due to condensation and coalescence with neighboring droplets until they become large enough to be removed by body forces (*e.g.*, gravity). Sliding and merging of large droplets clear portions of the cooled surface, allowing new primary droplets to form and grow from nucleation sites.

In dropwise condensation, heat from the condensation process transfers through the liquid-vapor interface (interfacial resistance $R_i'' = 1h_i$) and then conducts through the droplet to the cooled wall (R_{cond}) (Fig. 1). Internal circulation and convection within droplets is generally assumed negligible [9]. Interfacial heat transfer resistance is usually significant in dropwise condensation because the conduction length from the interface to the wall approaches zero at the contact line. Therefore, interfacial thermal resistance is dominant in the near-wall region. The relative overall contributions of interfacial and conduction resistances in droplet condensation heat transfer depend on the Biot number $\left(Bi = \frac{h_l r}{k_l}\right)$ and contact angle θ [10]. Average heat flux through the base of the droplet is given by the following relation:

$$q'' = \frac{\Delta T}{\frac{f(\mathrm{Bi},\theta) r}{k_l} + \frac{1}{2h_i}} \tag{1}$$

Here, q'' is the average heat flux through the base of the droplet, ΔT is the temperature difference between ambient vapor temperature and the base, r is the radius of curvature for the droplet, and k_l is the liquid-phase thermal conductivity. $f(\mathrm{Bi},\theta)$ is a scaling factor for the conduction contribution to overall droplet thermal resistance. f can be considered as an inverse fin efficiency for the droplet on the cooled wall, and should approach 0 for an infinitely conductive droplet ($\lim_{\mathrm{Bi}\to 0} f = 0$). Most prior studies assumed a constant factor $f = O(1)$ [8,11,12]. This assumption may be suitable for steady-state analyses where the distribution of drop sizes is constant. However, an effective average f value would still be specific

* Corresponding author at: 236A Reber Building, University Park, PA 16802, United States.
E-mail address: Alex.Rattner@psu.edu (A.S. Rattner).

http://dx.doi.org/10.1016/j.ijheatmasstransfer.2017.07.077
0017-9310/

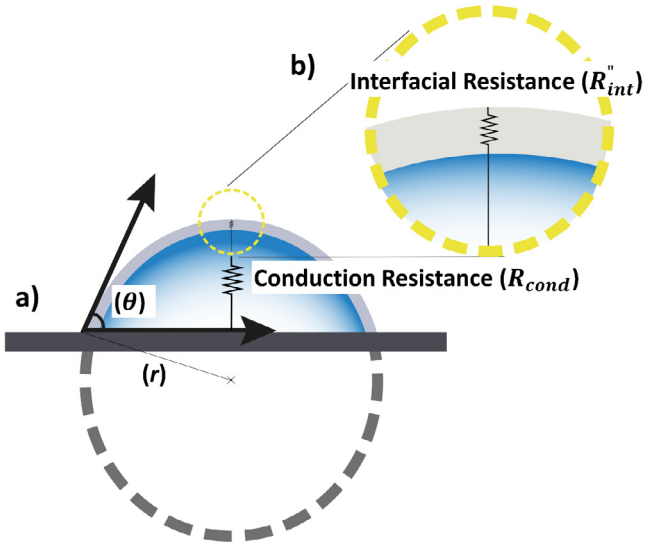

Fig. 1. (a) Schematic of the Droplet with radius r, contact angle θ, conduction resistance R_{cond} and interfacial resistance R_{int}. (b) Magnified view of the interfacial resistance.

to the operating conditions. For cases where the droplet size distribution evolves over time (*e.g.*, dropwise condensation startup), the variation of f as the droplet size distribution develops must be considered. Several studies have been performed to determine formulae for $f(\text{Bi}, \theta)$. Sadhal and Martin [13] and Kim and Kim [14] have proposed analytical models for hydrophilic surfaces ($\theta < 90°$). Recently, Miljkovic et al. [15] and Chavan et al. [16] have reported numerical and experimental results for hydrophobic surfaces ($\theta > 90°$). Generally valid models for $f(\text{Bi}, \theta)$ would facilitate dropwise condensation analyses, but are not currently available.

In this study, finite element heat transfer analyses are performed for 2958 cases to develop a single broadly applicable droplet condensation heat transfer formulation for $0.0001 \leqslant \text{Bi} \leqslant 1000$ and $10° \leqslant \theta \leqslant 170°$. Discretization errors are evaluated to determine uncertainty bounds for Richardson-extrapolated f factors. Results are validated against prior findings from Sadhal and Martin [13] and Chavan et al. [16]. Summarized data and simulation results from this study are publicly available at [17].

2. Modeling approach

In this study, finite element analyses are performed for heat transfer in sessile droplets using COMSOL MultiPhysics® (v. 5.2 [18]). In typical dropwise condensation conditions, >90% of the heat is transferred through droplets less than 200 μm in diameter [19]. Droplets in this size range are sufficiently small, such that Marangoni circulation and other convection effects can be neglected [20]. Therefore, conduction is the predominant mode of heat transfer. As droplets grow, the internal temperature distribution varies. However, the conduction-front propagation velocity $\left(\frac{\alpha_l}{r}\right)$ is generally much greater than the droplet growth rate $\left(\frac{dr}{dt}\right)$; therefore, the heat transfer process can be modeled as quasi-steady. For example, for a water droplet with 1 μm diameter and a 90° contact angle on a surface at 99.15 °C ($T_{sat} = 100.15$ °C) the conduction front velocity is $\frac{\alpha_l}{r} \sim 1.6 \times 10^{-1}$ ms^{-1}. Applying a standard droplet condensation heat transfer model (*e.g.*, from [11] with constant $f = 0.25$), the predicted growth velocity would only be $\frac{dr}{dt} = 8.4 \times 10^{-5}$ms^{-1} For similar conditions a 1 mm droplet will have $\frac{\alpha_l}{r} = 1.6 \times 10^{-4}$ms^{-1} and $\frac{dr}{dt} = 6 \times 10^{-7}$ms^{-1}. Based on these arguments, the in-droplet condensation heat transfer process reduces to conduction in a solid medium, with the following equation:

$$\nabla^2 T = 0 \tag{2}$$

For small droplets, as is the focus here, surface tension forces dominate gravity. Therefore, the droplets can be modeled as truncated spheres [16], and evaluated with 2-D axisymmetric domains (Fig. 2). A fixed temperature boundary condition is applied on the base of the axisymmetric droplet domain (1 K below the saturation temperature), representing the cooled condenser surface temperature. A convection boundary condition is applied to the liquid-vapor interface to account for interfacial resistance, with the following heat transfer coefficient [21]:

$$h_i = \left(\frac{2\sigma}{2-\sigma}\right) * \left(\frac{h_{lv}^2}{T_v v_l}\right) * \left(\frac{M}{2\pi R T_v}\right)^{1/2} \tag{3}$$

Here, h_i is the interfacial heat transfer coefficient, σ is the accommodation constant, h_{lv} is the enthalpy of vaporization, T_v is the ambient temperature, M is the molecular mass of the working fluid, and R is the specific gas constant. The saturation temperature of the vapor at the ambient pressure (T_{sat}) is substituted for T_v in Eq. (3).

The domain was meshed with nearly uniform size triangular elements (Fig. 2). The governing equation was discretized with second order accurate elements and solved to a relative residual of 10^{-14}. The total droplet heat transfer rates obtained from the FEA were used to determine $f(Bi, \theta)$, using the relation given in Eq. (1), for varying Biot number and contact angle values.

3. Simulation studies

A parametric study for droplet condensation heat transfer was performed. The contact angle (θ) was varied to span both the hydrophilic and hydrophobic regimes (10°–170°) in 10° increments. Droplet conductivity (k_l) was varied with fixed radius ($r = 1$ mm) and interfacial resistance ($h_i = 10{,}000$ W m^{-2} K^{-1}) to evaluate 174 Bi values from 0.0001 to 1000 for each contact angle. For water at atmospheric pressure, this Bi range spans droplet radii from 310 nm to 3.1 mm. In total, 2958 cases were studied.

Grid sensitivity studies were performed for each case with at least three meshes to extrapolate converged values of $f(\text{Bi},\theta)$ and corresponding uncertainties following the method of Celik et al. [22]. The technique is briefly described below.

Meshes (Fig. 2) with average element dimensions: $\Delta_3 = 2.2 \times 10^{-2}$ mm, $\Delta_2 = 1.2 \times 10^{-2}$ mm and $\Delta_1 = 6.0 \times 10^{-3}$ mm are employed. Subscript 3 refers to the coarsest mesh and subscript 1 refers to the finest mesh. The steps are as follows:

$$\varepsilon_{32} = f_3 - f_2; \quad \varepsilon_{21} = f_2 - f_1; \quad s = sgn\left(\frac{\varepsilon_{32}}{\varepsilon_{21}}\right) \tag{4}$$

$$R_{32} = \frac{\Delta_3}{\Delta_2}; \quad R_{21} = \frac{\Delta_2}{\Delta_1} \tag{5}$$

$$q(p) = \ln\left(\frac{R_{21}^p - s}{R_{32}^p - s}\right); \quad p(q) = \frac{\left|\ln\left(\left|\frac{\varepsilon_{32}}{\varepsilon_{21}}\right|\right) + q\right|}{\ln(R_{21})} \tag{6}$$

$$f_{ext} = (R_{21}^p f_1 - f_2)/(R_{21}^p - 1) \tag{7}$$

$$e_a^{21} = \left|\frac{f_1 - f_2}{f_1}\right|; \quad \text{GCI} = \frac{1.25 e_a^{21}}{R_{21}^p - 1} \tag{8}$$

$$unc = f_{ext} \times \text{GCI} \tag{9}$$